Chapter 18
Involvement of P_2X_7 Receptors and BDNF in the Pathogenesis of Central Poststroke Pain

Yung-Hui Kuan, Hsi-Chien Shih, and Bai-Chuang Shyu

Abstract Central pain is commonly found in patients with neurological complications that are associated with central nervous system insult, such as stroke. It can result directly from central nervous system injury. Impairments in sensory discrimination can make it challenging to differentiate central neuropathic pain from other types of pain or spasticity. Central neuropathic pain may also begin months to years after the injury, further obscuring the recognition of its association with past neurologic injury. This chapter focuses on the involvement of P_2X_7 receptor and brain-derived neurotrophic factor (BDNF) in central poststroke pain (CPSP). An experimental animal model is introduced that assesses the pathogenesis of central neuropathic pain, and pharmacological approaches and neuromodulatory treatments of this difficult-to-treat pain syndrome are discussed.

Keywords P_2X_7 receptor · Brain-derived neurotropic factor · Central poststroke pain · Cytokines · Thalamic hemorrhage · Medial thalamus · Anterior cingulate cortex

18.1 Central Neuropathic Pain

The International Association for the Study of Pain defines neuropathic pain as pain that is caused by a lesion or disease of the somatosensory nervous system [1]. Neuropathic pain resulted from origins that affect the central nerves system (CNS) termed central neuropathic pain, which can result from any type of injury to the CNS. Central neuropathic pain is most commonly a sequela of stroke, multiple sclerosis, or SCI [2]. Central neuropathic pain is often found months or years after the original insult to CNS, which is very challenging to treat and may not respond

Y.-H. Kuan · H.-C. Shih · B.-C. Shyu (✉)
Division of Neuroscience, Institute of Biomedical Sciences, Academia Sinica, Taipei, Taiwan
e-mail: bmbai@gate.sinica.edu.tw

B.-C. Shyu, M. Tominaga (eds.), *Advances in Pain Research: Mechanisms and Modulation of Chronic Pain*, Advances in Experimental Medicine and Biology 1099, https://doi.org/10.1007/978-981-13-1756-9_18

to pharmacological agents that are routinely used for peripheral neuropathic pain. Thus, understanding the pathogenesis of different central neuropathic pain is thus a vital task for medical researchers, physicians, and specialists.

18.2 Central Poststroke Pain

Stroke is one of the top five causes of death in the United States [2, 3] and responsible for 1 in 20 deaths [2, 4]. Stroke is also one of the leading causes of disability in the United States [2, 5]. Central poststroke pain (CPSP) is a neuropathic pain syndrome that is associated with somatosensory abnormalities following stroke and the most common form of central neuropathic pain [6, 7]. Because of the difficulty managing the condition and potential under diagnosis, studies that address detailed mechanisms of CPSP are not well established, thus resulting in limited treatment options [8, 9].

Articles have reported that the lateral and medial pain pathways have been shown to rule the homeostasis of pain processing in coding the strength of CPSP [10–13]. Reports have shown that stroke patients with dysfunction in the lateral thalamus exhibited a disruption of inhibition of signaling to the medial thalamus (MT), resulting in mechanical allodynia and thermal hyperalgesia [14, 15], which can be viewed as a disinhibition disorder.

The descending pain modulation system, including the dorsolateral prefrontal cortex, rostral anterior cingulate cortex (ACC), amygdala, hippocampus, periaqueductal gray (PAG), and rostral ventromedial medulla, comprises a network that regulates nociceptive processing [16]. Human functional magnetic resonance imaging (fMRI) studies have provided important evidence that the spinothalamic tract (STT) and MT-ACC pathway might be involved in CPSP [17–20]. A recent human fMRI study dissociated differences in thalamic subregions in CPSP reporting that the VPL but not VMpo plays a crucial role in CPSP [27]. Another fMRI study indicated that the contralateral somatosensory cortex and bilateral mid-/posterior insula, anterior insula, and posterior cingulate were activated during exposure to acute pain stimulation [20], concluding that the STT and MT-ACC pathway may be critically involved in CPSP symptoms.

18.3 Animal Model of CPSP

To assist the understanding of CPSP, development and characterization of animal models that mimic CPSP is the first hurdle to discovering the underlying mechanisms of this disease and possible therapeutics. Following in this section, we introduce the development of an animal model of CPSP. We will discuss our observations with studies that utilized this model of a lateral thalamic hemorrhage in rats to generate CPSP, which we believe is useful for studying the neuropathology and

physiology of CPSP and developing potential therapies. We will also discuss our findings of studies that utilized the same animal model of CPSP focusing on the involvement of P_2X_7 receptors and brain-derived neurotrophic factor (BDNF) in poststroke inflammation and the pathophysiology of CPSP.

18.4 Preparation of Animal Model of CPSP with Targeting ATP and BDNF Receptors

Male Sprague Dawley rats (250–300 mg) from laboratory animal suppliers were utilized. All surgical procedures were performed according to previously described methods [21] with slight modifications. Experimental rats were maintained under anesthesia with 1% isoflurane during surgery. Body temperature was maintained at 36.5–37.5 °C with a homeothermic blanket system, and the animals were injected with type IV collagenase (0.125 U/0.5 μl saline) in the region of right ventral posterior medial nucleus (VPM)/ventral posterior lateral nucleus (VPL) of the thalamus (coordinates: 3.0–3.5 mm posterior, 3.0–3.4 mm lateral to bregma, 5700–6000 μm depth). Sham control animals were injected with 0.5 μl sterile saline only. An intravenous catheter was implanted in the femoral vein, tunneled subcutaneously, and fixed to the back for chronic perfusion of the P_2X_7 receptor antagonist Brilliant Blue G (BBG; 50 mg/kg), began 6 h after hemorrhagic lesion induction, once daily for the following 3 days and a total of four times. To investigate effects of BDNF in vivo, the rats received an acute microinjection of artificial cerebrospinal fluid (1 μl/min), denatured TrkB-Fc (dTrkB-Fc, 1 μg/μl/min), and TrkB-Fc (1 μg/μl/min), with a 30 gauge stainless-steel cannula in the MT (2.5 mm posterior, 1.5 mm lateral to bregma, 4.2 mm depth) during electrophysiological recording under isoflurane anesthesia. For the group of rats that received chronic microinjections under awake conditions, a 27 gauge stainless-steel cannula was implanted in the VB (2.5 mm posterior, 2.5 mm lateral to bregma, 5.2 mm depth) and conglutinated with dental resin under the same anesthetic conditions. On day 36, dTrkB-Fc, TrkB-Fc (1 μg/μl/day), or Tat cyclotraxin-B (CTX-B; 0.5 μl solution, 10 μg/μl/day; Tocris, Bristol, United Kingdom) was applied at a rate of 0.3 μl/min per injection using a 30 gauge stainless-steel cannula in the VB once daily followed by a 5-day rest period (days 36–40).

18.5 Behavioral Tests that Are Typically Performed to Evaluate CPSP Conditions

18.5.1 von Frey Test

The animals were placed on an elevated mesh platform for 30 min before testing, and filaments were gradually applied with ascending, graded force to determine the minimal force that elicited a limb withdrawal response. The threshold was defined

as the average of three minimal forces that were measured in consecutive trials, each separated by 5 min.

18.5.2 Plantar Test

The plantar test was performed by placing the rats in a transparent Plexiglas box for 30 min before testing. Radiant heat (IITC 390G Plantar Test, IITC Life Science, Woodland Hills, CA, USA) was delivered through the glass floor. Before each test, the heat-generating apparatus was calibrated to the same power level. The hindpaw was directly stimulated by the infrared light source to assess withdrawal responses. The paw-withdrawal latency in response to thermal stimulation was measured. Each rat was tested in three trials with the right and left hindpaws, respectively. The inter-trial interval was 5 min.

18.6 Electrophysiological Recordings to Observe Neuronal Activity

Electrophysiological recordings were performed 5 weeks after CPSP induction. The rats were maintained under anesthesia with 1.5% isoflurane. Multichannel probes (NeuroNexus) were used to record extracellular field potentials in the right ACC (2.5 mm anterior, 1 mm lateral to bregma) and right MT (2.2–3.5 mm posterior, 0.5–1.0 mm lateral to bregma). An Ag–AgCl reference electrode was placed in the nasal cavity. The left sciatic nerve was isolated and implanted with a cuffed electrode to deliver constant-current pulses (Model 2100, A-M Systems) for sciatic nerve stimulation (SNS). The minimal effective pulse was measured as the 1 × threshold stimulation for each experimental animal. Neuronal activity in the MT was recorded using 2-, 5-, 10-, and 20-fold increases in the threshold current. The sampling rate of the recorded analog signals was 6 kHz for the field potential data and 24 kHz for the unit data. All of the electrophysiological data were processed using a multichannel data acquisition system (Tucker-Davis Technologies).

18.7 Immunostaining and Cell Count Analysis to Evaluate Changes in Tissue Composition

After electrophysiological recording, the animals were sacrificed and transcardially perfused with 4% paraformaldehyde in phosphate-buffered saline, and the brains were removed and postfixed overnight at 4 °C. The brains were incubated with a

30% sucrose solution prior to cryosectioning (30–40 μm sections). The ACC, primary somatosensory cortex (S1), MT, and VPL/VPM cryosections were divided into three sets. One set of sections was stained with cresyl violet, and the other two sets were stained with the following primary antibodies: rabbit anti-P2X7 (1:50, ATTO-550, Alomone Labs) and mouse anti-CD11b (1:100, Serotec), followed by secondary Alexa Fluor-488 goat anti-mouse IgG (H + L) antibody (1:400, Life Technologies) and DAPI staining (1 μg/ml, Life Technologies).

After immunohistochemistry, four sections with visible lesions from the center were chosen for image analysis. Stacks of images at 2 μm increments in depth were collected using a confocal microscope (LSM780, Zeiss) with Zen software (Zeiss) and either a 20× air objective (NA 0.7) for automatic full-section scans or 40× oil objective (NA 1.3–1.4) for small-field single-cell distinguishable images. The continual disruption of tissue organization and/or the loss of staining were identified as the lesion area. The edges of the lesion were marked in individual sections, and 200 μm distances from the edges of the lesion were chosen as the distant field, the area of which (μm^2) was the region of interest (ROI), measured using ImageJ software with calibrated parameters from the image acquisition. Signals >15 μm accompanied by a DAPI signal were counted as positive signals. The cell counts were manually performed within the distant field using ImageJ 1.47 software (National Institutes of Health).

18.8 Gene Transcript Analysis: Reverse-Transcription Polymerase Chain Reaction for the Determination of Selected Cytokines and Neurotropic Factor

RNA samples from sham control and CPSP rat brain tissues from peri-lesion sites were collected and processed with designed probes that flanked rat tumor necrosis factor α (TNF-α), IL-6, IL-1β, and BDNF for reverse transcription polymerase chain reaction (RT-PCR). Crude extracts of total RNA were obtained from each experimental animal using Trizol reagent (Invitrogen). Reverse transcription was performed with 0.5 μg total RNA using designed probes and Superscript III (Invitrogen) in a 20 μl reaction mixture. Quantitative PCR amplification was performed for all of the samples in a reaction volume of 50 μl that contained 1 × standard PCR buffer and 1 U Platinum *Taq* DNA polymerase (Invitrogen). The quantitative PCR product samples were analyzed using agarose gel electrophoresis. Each experiment is consisted of TNF-α, IL-6, IL-1β, and BDNF targets and was performed in triplicate. The internal sham controls consisted of GAPDH, and negative sham controls consisted of the omission of the reverse transcriptase reaction or no cDNA template.

18.9 Digital Data Processing and Statistical Analysis

All of the electrophysiological data were transformed and processed using MATLAB (MathWorks). Prominent evoked oscillations based on the method for the current source density (CSD) analysis of evenly spaced multichannel extracellular field potentials were used to display the evoked ACC response [22]. Unit activity that was recorded from the MT was digitally filtered to obtain high-frequency spike activity in response to SNS. All of the statistical data were analyzed using unpaired Student's *t*-tests, one-way analysis of variance (ANOVA), and two-way ANOVA using SPSS software. Values of $p < 0.05$ were considered statistically significant.

18.10 CPSP Features and Molecules that may Effectively Modulate CPSP Conditions

18.10.1 CPSP Rats Exhibit Allodynia and Hyperalgesia, Which are Eliminated by P_2X_7 Receptor Antagonism and BDNF Receptor Blockade

Rats with thalamic lesions developed significant hyperalgesia to mechanical and thermal pain stimulation beginning 1 week after surgical CPSP induction, which persisted for at least 5–6 weeks compared with the control group (Fig. 18.1).

18.10.2 CPSP Rats Exhibit Elevated CD11b, P_2X_7 Receptor, Selected Cytokine, and BDNF Levels in Peri-lesion Sites

Increases in the immunoreactivity of the reactive microglia marker CD11b and P_2X_7 receptors were found largely in peri-lesion sites in CPSP rats, whereas their immunoreactivity remained at basal levels in the contralateral site (data not shown) and sham control rat brains. Significant increases in the counts of cells that were immunoreactive to both CD11b and P_2X_7 receptors were observed in selected regions of interest (ROI; Fig. 18.2).

Fig. 18.1 (continued) time points with the CPSP groups (showing contralateral hindpaw data only: $n = 25$; $^{**}p < 0.01$, $^{*}p < 0.05$, two-way ANOVA followed by Tukey post hoc test). (**e**) Changes in mechanical (left) and thermal (right) thresholds after microinjections of dTrkB-Fc, TrkB-Fc, and CTX-B in CPSP animals. $^{\#}p < 0.05$, control-TrkB-Fc group compared with CPSP-TrkB-Fc group or CPSP-CTX-B group (mixed two-way ANOVA followed by post hoc test): $^{\#}p < 0.05$, control-TrkB-Fc group compared with CPSP-dTrkB-Fc group (mixed two-way ANOVA followed by post hoc test). (Figure adapted or modified from (**a**–**c**) Kuan et al. [38] (**d**) Kuan et al. [39, 40], and (**e**) Shih et al. [41])

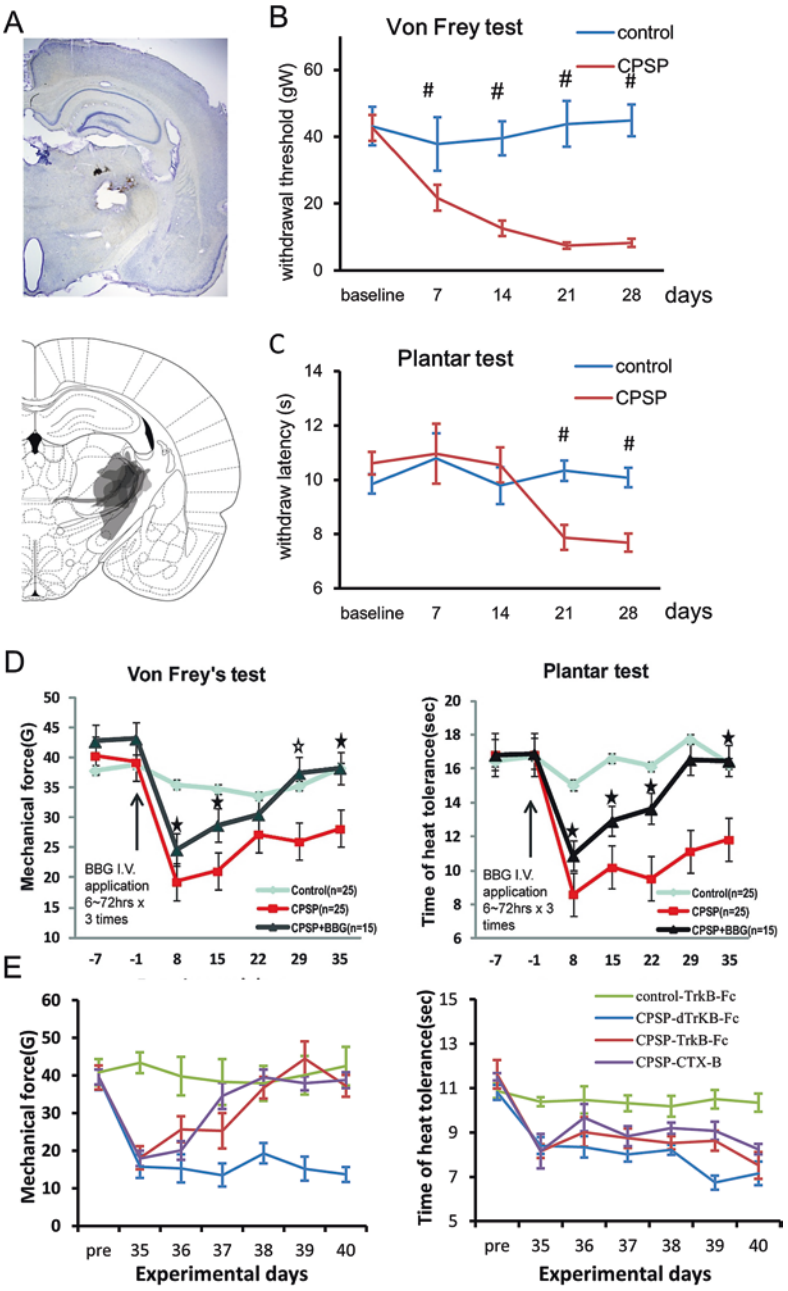

Fig. 18.1 CPSP rats exhibit allodynia and hyperalgesia, which were eliminated by P_2X_7 receptor antagonism and BDNF receptor blockade. (**a**) One month post-thalamic hemorrhage induction, a lesion scar or hollow space remained. One week after the lesion, the mechanical von Frey test (**b**) and thermal plantar test (**c**) of allodynia were performed once a week for 5 weeks. (**d**) Effects of BBG treatment on von Frey test (left) and plantar test (right) in both hindpaws compared with corresponding

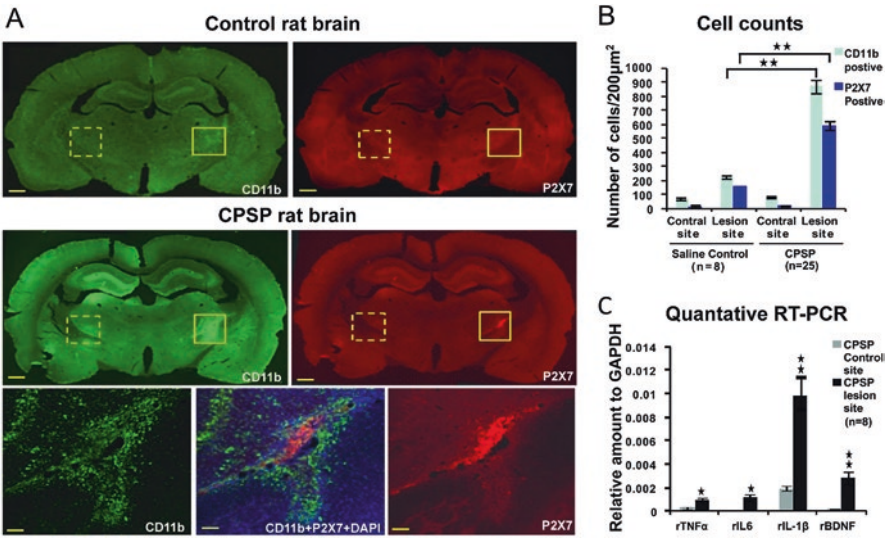

Fig. 18.2 CPSP rats exhibit elevated CD11b, P_2X_7 receptor, selected cytokines, and BDNF levels in peri-lesion sites. (**a**) Immunofluorescent analysis of CPSP rat brains. (*Upper panel*) The control rat brain had only slight elevations of the reactive microglia marker CD11b (left, *green*) and normal basal levels of P_2X_7 receptors (right, *red*). (*Middle panel*) CPSP rat brain with significantly elevated levels of the reactive microglia marker (*green*) and P_2X_7 receptor (*red*) along the lesion site around the right VPM/VPL of the thalamus. (*Lower panel*) Overlapped enhancement of CD11b and P_2X_7 receptors around the lesion site under higher magnification. Scale bar = 500 μm for upper and middle panels, 50 μm for lower panel. Solid-line square, peri-lesion site on the right. Dashed-line square, control site on the left. (**b**) Quantification of CD11b and P_2X_7-positive cells. The ROI of each brain slice was selected as the squares on the right and left sides that are shown in Fig. 18.2a. $^{**}p < 0.01$, compared with corresponding parameter in control group. (**c**) Quantitative RT-PCR results of selected cytokines (TNF-α, IL-6, IL-1β) and BDNF. The levels of these cytokines were elevated in CPSP rat brains compared with control brains ($F_{3,16} = 28.324$, $^{*}p < 0.05$, $^{**}p < 0.01$, two-way ANOVA followed by Tukey post hoc test). (Figure adapted or modified from Kuan et al. [39, 40])

18.10.3 CPSP Rats Exhibit Enhancement of the Noxious Response in the MT-ACC Pathway, Which was Suppressed by P_2X_7 Receptor Antagonism and BDNF Receptor Blockade

Thalamocingulate circuitry in the CNS is known as a medial pain processing pathway. Changes in nociceptive sensitivity in the forebrain under conditions of neurogenic pain likely result from aberrant neuronal activity along this pathway, reflected by thalamocortical dysrhythmia [23–26]. To test the hypothesis that persistent pain in CPSP rats is accompanied by changes in nociceptive sensitivity, multichannel electrodes were used to record evoked neuronal activity in the ACC and MT in response to SNS. Our study found that CPSP rats exhibited enhancement of the noxious response in the MT-ACC pathway, which was suppressed by a P_2X_7 receptor antagonist and BDNF receptor blocker (Fig. 18.3).

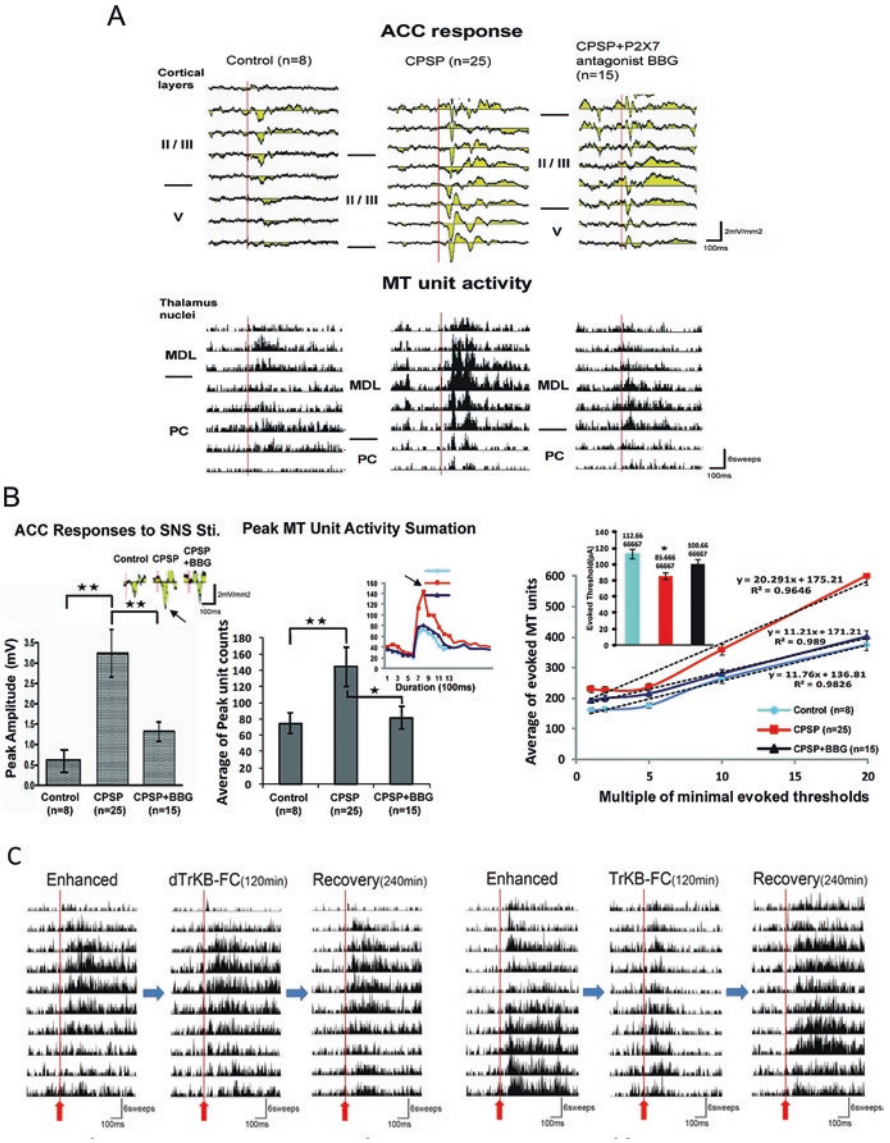

Fig. 18.3 CPSP rats exhibit enhancement of the noxious response in the MT-ACC pathway, which was suppressed by P_2X_7 receptor antagonism and BDNF receptor blockade. (**a**) Representative traces of evoked ACC CSD and MT unit activity following SNS. CPSP rats exhibited a stronger response to SNS. BBG-treated CPSP rats had a lower CSD and lower MT unit activity compared with the previously tested CPSP rats. (**b**) Quantification of ACC and MT neuronal activity in control rats and CPSP rats with and without BBG treatment. BBG-treated CPSP rats exhibited a significantly lower CSD peak amplitude (inset, arrow) of the ACC sink current and integrated MT unit activity (inset, arrow) compared with CPSP rats. One-way ANOVA followed by Tukey *post hoc* test: $*p < 0.05$, $**p < 0.01$, $F_{2,38} = 38.221$ (left panel), $F_{2,38} = 29.245$ (right panel). (**c**) Influence of BDNF and BDNF scavenger TrkB-Fc injection in the MT. Noxious responses were recorded in CPSP animals. The wind-up noxious response was not influenced by dTrkB-Fc. One to 2 h after the TrkB-Fc injection, the enhanced noxious response in the MT decreased and recovered after 180–240 min. (Figure adapted or modified from (**a**, **b**) Kuan et al. [39, 40] and (**c**) Shih et al. [41])

18.10.4 CPSP Rats Exhibit Enhancement of Spontaneous MT Activity, Which was Suppressed by BDNF Receptor Blockade

In our studies, we also observed significant changes in spontaneous electroencephalographic activity in CPSP rats, which strongly indicated the manifestation of persistent pain-related behavior. BDNF levels were not reduced by treatment with the P_2X_7 receptor antagonist BBG. This indicates the involvement of a separate BDNF-mediated mechanism in CPSP. To examine the influence of BDNF after CPSP, the BDNF scavenger TrkB-Fc was infused into the MT. Denatured TrkB-Fc (dTrkB-Fc) was infused in the control group. The evoked response in the MT was not significantly altered by dTrkB-Fc in control rats. TrkB-Fc infusion for 60–120 min attenuated the MT evoked response, which then recovered after 240 min. Both the fast component and late component significantly decreased after TrkB-Fc infusion (Fig. 18.4).

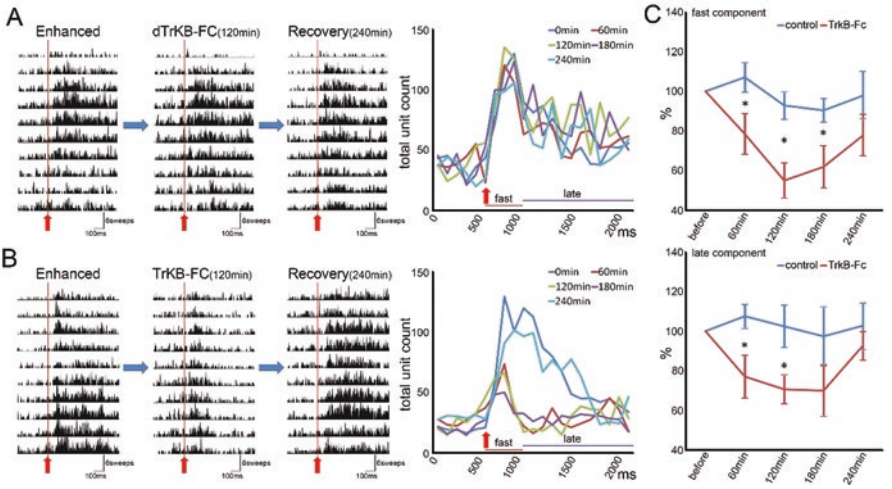

Fig. 18.4 CPSP rats exhibit enhancement of spontaneous medial thalamus activity, which was suppressed BDNF receptor blockade. (**a**) The enhanced MT nociceptive response was not influenced by the injection of denatured TrkB-Fc at any time period of the 240-min recording. Summed numbers of MT multiunit response before and after the injection at different time periods were not significantly different. The stimulation time was at 600 ms (red arrow). The overall recording period was 2100 ms. The summed time bin was 100 ms. (**b**) Sixty minutes (at 120 min) after the TrkB-Fc injection, the enhanced MT nociceptive response on CPSP decreased, and the enhanced nociceptive response recovered after 240 min. (**c**) Effect of denatured TrkB-Fc or TrkB-Fc treatment on the fast component and late component of evoked MT nociceptive responses. Four hours after the injection, the fast component (between 90.4 ± 5.8% and 107.1 ± 7.1%) and late component (between 97.4 ± 10.4% and 107.6 ± 5.8%) were not influenced by denatured TrkB-Fc. The fast component (5.0 ± 8.6% at 120 min, 61.9 ± 10.4% at 180 min) and late component (between 70.7 ± 7.0% at 120 min) significantly decreased after the TrkB-Fc injection. Fast component: $F_{1,10} = 6.69$, $^*p < 0.05$ at 60, 120, and 180 min (mixed two-way ANOVA followed by post hoc test). Late component: $F_{1,10} = 4.62$, $^*p < 0.05$ at 60 and 120 min (mixed two-way ANOVA followed by post hoc test). (Figure adapted or modified from Shih et al. [41])

18.10.5 P2X7 Antagonism and BDNF Receptor Blockade Prevented or Reversed the High Coherence Coefficients of MT-ACC Spontaneous Local Field Potentials in CPSP Rats

Persistent pain states under conditions of neurogenic pain may result from "thalamocortical dysrhythmia" [26]. Evaluating the effects of BBG and TrkB-Fc treatments on alterations of spontaneous cortical EEG oscillations helps to study such phenomena. Local field potentials in the ACC were evaluated in control rats, CPSP rats, and CPSP rats that were either treated with the P_2X_7 receptor antagonist BBG or received an intra-MT injection of the BDNF receptor blocker TrkB-Fc (Fig. 18.5).

18.10.6 Involvement of P_2X_7 and BDNF in Different Series of Sequential Signaling Effects on Microglia and Neuronal Activity in CPSP Rats

Combined our studies and other reports of the post-tissue damage signaling response, we postulated the net involvement of P_2X_7 receptors and BDNF, a schematic diagram of cellular mechanisms that are hypothesized to underlie the pathophysiology of CPSP is shown in Fig. 18.6.

18.11 Conclusion

This chapter described a particularly common type of central neuropathic pain, CPSP, and discussed the effects of treatment with a P_2X_7 receptor antagonist and BDNF receptor blocker on nociceptive behaviors and aberrant neuronal activity in the thalamocingulate pathway. Notably, the early targeting of P_2X_7 receptors could act as an immunosuppressant that inhibited inflammatory damage to brain tissue and prevented the occurrence of CPSP as the application of P_2X_7 receptors antagonist reduced the CPSP elevation of inflammatory cytokines. The alterations of thalamic neuronal excitability in CPSP could be rescued by treatment with a BDNF receptor blocker. Both P_2X_7 receptor antagonism and BDNF receptor blockade altered abnormal spontaneous EEG activity and coherence, which are strongly indicative of thalamocortical dysthymia.

A rat model of CPSP has been successfully applied in several studies and shown to be useful for elucidating the underlying causes of CPSP that are associated with lateral thalamic lesions. CPSP rats exhibited persistent sensitized behaviors with lower thresholds and greater neuronal responses to noxious stimulation and alterations of spontaneous EEG patterns within various frequency bands. This model consists of brain tissue damage, and its wound progression causes innate inflammatory

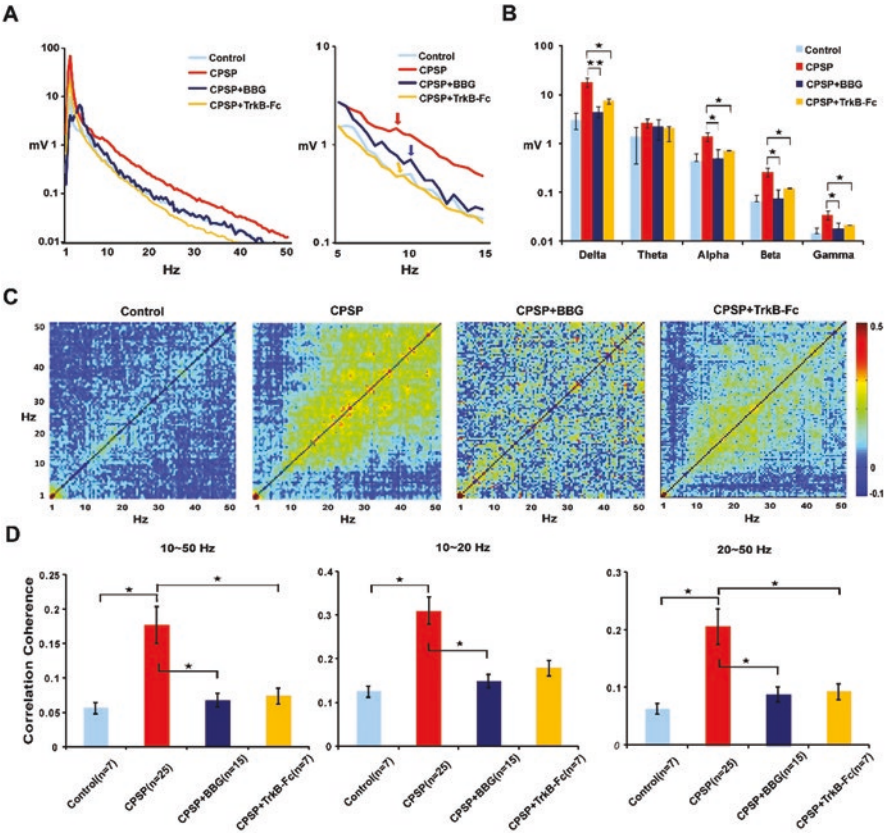

Fig. 18.5 P_2X_7 receptor antagonism and BDNF receptor blockade prevented or reversed high coherence coefficients of MT-ACC spontaneous local field potentials in CPSP rats. (**a**) Averaged power density of local field potentials (LFPs) shown in left panel in control group (light blue line, $n = 7$), CPSP group (red line, $n = 25$), CPSP+BBG group (dark blue line, $n = 15$), and CPSP+TrkB-Fc group (yellow line, $n = 7$). Averaged LFP spectrum peaks in CPSP+BBG group and CPSP+TrkB-Fc group revealed a shift that was similar to the frequency spectrum in the control group. (**b**) The enhanced spontaneous LFP oscillation in the CPSP+BBG group and CPSP+TrkB-Fc group was shifted similarly to the control group in the alpha, beta, and gamma bands ($F_{3,27} = 11.16$, 9.20, 7.56, 8.29, 9.24 for delta, theta, alpha, beta, and gamma bands, respectively, $^*p < 0.05$, $^{**}p < 0.01$, one-way ANOVA followed by Tukey post hoc test). (**c**) Color maps of averaged correlation coherence for spontaneous LFP oscillation between 10 and 50 Hz differed in the CPSP group. BBG and TrkB-Fc treatments shifted the LPF correlation coherence similarly to control animals (control, $n = 7$; CPSP, $n = 25$; CPSP+BBG, $n = 15$; CPSP+TrkB-Fc, $n = 7$). (**d**) Comparisons of averaged LFP correlation coherence values between 10 and 50 Hz, 10 and 20 Hz, and 20 and 50 Hz. (*Left panel*) Mean value of correlation coefficient between 10 and 50 Hz in the control group (0.056 ± 0.015, $n = 7$), CPSP group (0.177 ± 0.021, $n = 25$), CPSP+BBG group (0.067 ± 0.019, $n = 15$), and CPSP+TrkB-Fc group (0.074 ± 0.020, $n = 7$). (*Middle panel*) Mean value of correlation coefficient between 10 and 20 Hz in the control group ($r = 0.125 \pm 0.024$, $n = 7$), CPSP group ($r = 0.31 \pm 0.046$, $n = 25$), CPSP+BBG group ($r = 0.149 \pm 0.036$, $n = 15$), and CPSP+TrkB-Fc group ($r = 0.135 \pm 0.032$, $n = 7$). (*Right panel*) Mean value of correlation coefficient between 20 and 50 Hz in the control group ($r = 0.073 \pm 0.015$, $n = 7$), CPSP group ($r = 0.206 \pm 0.03$, $n = 25$), CPSP+BBG group ($r = 0.088 \pm 0.023$, $n = 15$), and CPSP+TrkB-Fc group ($r = 0.093 \pm 0.023$, $n = 7$). Different band ranges were analyzed separately by one-way ANOVA ($^*p < 0.05$). (Figure adapted or modified from Kuan et al. [39, 40] and Shih et al. [41])

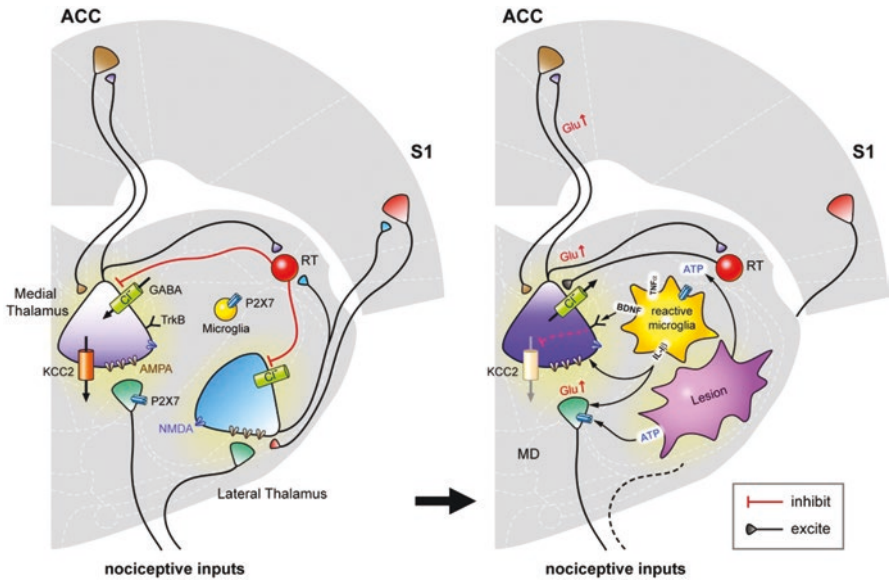

Fig. 18.6 Schematic illustration of P_2X_7 receptor and BDNF involvement in different series of sequential signaling effects on microglia and neuronal activity in CPSP. Combining our data, we postulate that, in a normal physiological state, P_2X_7 receptors are found on glutamatergic nerve terminals and microglial cells in the central nervous system. Glutamate that is released by neuron bursting is partially removed by transporters on adjacent astrocyte processes and also excites AMPA receptors on these processes, which then release ATP. The remaining ATP acts on presynaptic P_2X_7 receptors to facilitate glutamate release in the absence of neuropathic/neuroinflammatory insult. The positive feedback of terminal glutamate release that triggers astrocyte ATP release and leads to further glutamate release through the activation of P_2X_7 receptors is then sufficient to allow normal action potentials to elicit postsynaptic action potentials. Basal BDNF levels do not alter ionic flow through KCC2 channels and GABA receptors via TrkB receptor modulation. In a pathological state, such as CPSP, these traumatized cells at the lateral thalamic lesion site release a high amount of intracellular ATP, and a higher amount of BDNF and IL-1β is secreted by reactive microglia into the surrounding tissues, including synaptic clefts. Subsequently, ATP and IL-1β enhance glutamate release, resulting in a higher frequency of neuron bursting along the thalamocingulate pathway. Elevated BDNF levels result in overbinding to TrkB receptors, thus inducing the downstream inhibition of KCC2 and inversion of the flow of chloride ions through the GABA receptor, which then contributes to the disinhibition of lateral thalamus inhibitory inputs to the medial thalamus. This effect also results in a higher frequency of neuron bursting along the thalamocingulate pathway. After the onset of CPSP, P_2X_7 receptor antagonism can block presynaptic P_2X_7 receptor activation, and BDNF blockade may reduce the disinhibition, resulting in the efficient suppression of the hyperexcitability of MT and ACC neurons in response to nociceptive stimulation. The early targeting of P_2X_7 receptors upon the occurrence of stroke may block the overexpression of activated microglia and prevent the greater release of IL-1β, thus resulting in the prevention of CPSP. (This diagram adapted or modified from Kuan et al. [39, 40] and Shih et al. [41])

responses that may reflect the initiation of persistent pain. Electrophysiological assessment along the thalamocingulate nociceptive pathway provides solid neurological evidence that MT neuron hyperexcitability and greater cingulate responses may underlie the hyperalgesia and reduction of exploratory movements that are observed in nociceptive pain-related behavior. Abnormal thalamic bursting activity was observed in patients who suffered from central pain, and an imbalance of the lateral and medial thalamic interaction was proposed [27, 28]. The present chapter reports profound changes in the threshold and sensitivity of thalamic and cortical responses and spontaneous cortical EEG, strongly supporting the hypothesis that the deafferentation that results from lateral thalamic lesions may alter medial thalamic neuronal excitability [28, 29]. The alterations of spontaneous EEG patterns in conditions of CPSP suggest that both cingulate cortical and thalamic neurons in the medial pain pathway may contribute to persistent pain-related behavior, manifested as alterations of locomotor activity and neurogenic central pain that results from thalamocortical dysrhythmia, as proposed by Llinás [23].

P_2X_7 receptor expression was elevated in CPSP brains at peri-lesion sites and associated with CNS immunoresponsive cells (i.e., reactive microglia). The adenosine triphosphate (ATP)-induced activation of P_2X_7 receptors led to the rapid maturation and release of IL-1β from proinflammatory microglia suggesting that activation of this ATP receptor after hemorrhage plays an important role in the progression of CPSP [30]. Combining that the P_2X_7 receptor activation have been reported to facilitate the release of glutamate by mobilizing Ca^{2+} in the terminals [31–33] and the progression of this persistent pain could be regulated by inhibition of P_2X_7 receptors, we thus postulate, such phenomena may result from the prevention of ATP activation and thus lead to a reduction of glutamatergic facilitation, hence preventing the further release of proinflammatory cytokines, particularly IL-1β. The BBG treatment approach shortly after stroke induction may prevent excessive inflammation and the resulting hyper-release of cytokines from sites of trauma. Thus, the early targeting of P_2X_7 receptors after neuronal injury may have neuronal protection effects [34]. These results support our hypothesis and lead us to conclude that the CPSP condition is linked to the activation of P_2X_7 receptors through the release of abundant intracellular ATP to the extracellular space following thalamic cell damage. The increase in intracellular ATP levels then facilitates nociceptive input signals along the thalamocingulate pathway, thus chronically enhancing innate inflammation that is caused by IL-1β secretion.

In addition to the involvement of P_2X_7 receptors in the increase in nociceptive responses in the thalamocingulate pathway, our studies also found that BDNF mediates thalamic hypernociceptive responses in CPSP. The BDNF mRNA in the MT increased after CPSP, and the MT nociceptive responses were inhibited by an acute injection of BDNF receptor blocker into the MT.

The shift of low-frequency bands and increase in the EEG correlation coefficient in neurological patients with chronic pain was reported to be caused by thalamocortical dysrhythmia oscillation [35, 36]. The abnormal cortical oscillation pattern was thought to be attributable to over-enhancement of the GABA system in the thalamus [26, 37]. Consistent with this possibility, we found that the role of the GABA system

is altered in CPSP (data not shown). Characteristics of EEG oscillation patterns and coherence coefficients in the CPSP group were highly similar to CPSP patients [23, 26, 29]. The results of TrkB-Fc treatment confirmed that an alteration of the GABAergic system could be one of the main reasons for thalamocortical dysrhythmia. The high correlation coefficient between 10 and 50 Hz in CPSP animals was completely abolished by BBG treatment indicating that P_2X_7 receptor antagonism may alter glutamatergic transmission. This brought hints of that the glutamatergic system may also play an important role in thalamocortical dysrhythmia oscillation after CPSP. The abolishment of correlation coefficient between 20 and 50 Hz was differed between the effect of $P2X_7$ receptor or BDNF, such differed effects of BBG and TrkB-Fc treatments on CPSP thalamocortical dysrhythmia indicate that the mechanisms of P_2X_7 receptors and BDNF are different in CPSP.

The animal model of CPSP that was introduced in this chapter has strong preclinical value. It opens insights into drugs that target P_2X_7 receptors and BDNF receptors that may be applied clinically as either early treatments at the initial onset of stroke or delayed treatments until the generation of CPSP in the subacute to chronic phase. For stroke patients who already suffer from CPSP, our results also indicate that targeting P_2X_7 receptors and BDNF TrkB receptors may have antinociceptive effects by suppressing or blocking neuronal hyperexcitability and reversing abnormal oscillations. The cell count results demonstrated that the early treatment of stroke patients with a P_2X_7 receptor antagonist can prevent the activation of microglial P_2X_7 receptors in peri-lesion tissue, thus reducing the release of regional inflammatory cytokines and associated neuronal damage. Our preliminary tests have shown that both site-directed and systemic infusions of the BNDF receptor blocker BBG did not have apparent toxicity in experimental animals, suggesting its potential as a clinical therapeutic candidate in acute stroke or other brain injury.

Acknowledgment We thank the Taiwan Mouse Clinics for their suggestions on the behavioral tests. We are thankful for the technical support from the Neural Circuit Electrophysiology Core at Academia Sinica. The present study was supported by grants from the Ministry of Science and Technology to Dr. Bai-Chuang Shyu (105-2325-B-001-010, 105-2320-B-001-025-MY2, and 106-2321-B-001-043). This work was conducted at the Institute of Biomedical Sciences, which received funding from Academia Sinica.

References

1. International Association for the Study of Pain. IASP taxonomy. Retrieved from: http://www.iasp-pain.org/Taxonomy#Neuropathicpain. Updated October 6, 2014. Accessed 27 Mar 2018
2. Watson JC, Sandroni P (2016) Central neuropathic pain syndromes. Mayo Clin Proc 91(3):372–385
3. Centers for Disease Control and Prevention. FastStats: leading causes of death. Updated September 30, 2015. Retrieved from: http://www.cdc.gov/nchs/fastats/leading-causes-of-death.htm. Accessed 27 Mar 2018
4. Benjamin EJ, Virani SS, Callaway CW, Chamberlain AM, Chang AR, Cheng S et al (2018) Heart disease and stroke statistics-2018 update: a report from the American Heart Association. Circulation 137(12):e67–e492

5. Centers for Disease Control and Prevention (2009) Prevalence and most common causes of disability among adults: United States, 2005. Morb Mortal Wkly Rep 58(16):421–426
6. Tasker RR (2004) Central pain states. In: Warfield CA, Bajwa ZH (eds) Principles and practice of pain medicine, 2nd edn. McGraw-Hill, New York, pp 394–404
7. Bowsher D (1996) Central pain: clinical and physiological characteristics. J Neurol Neurosurg Psychiatry 61(1):62–69
8. Bowsher D (2001) Stroke and central poststroke pain in an elderly population. J Pain 2:258–261
9. Kumar G, Soni CR (2009) Central post-stroke pain: current evidence. J Neurol Sci 284:10–17
10. Wang G, Thompson SM (2008) Maladaptive homeostatic plasticity in a rodent model of central pain syndrome: thalamic hyperexcitability after spinothalamic tract lesions. J Neurosci 28(46):11959–11969
11. Su YL, Huang J, Wang N, Wang JY, Luo F (2012) The effects of morphine on basal neuronal activities in the lateral and medial pain pathways. Neurosci Lett 525(2):173–178
12. Zhang Y, Wang N, Wang JY, Chang JY, Woodward DJ, Luo F (2011) Ensemble encoding of nociceptive stimulus intensity in the rat medial and lateral pain systems. Mol Pain 7:64
13. Martin RJ, Apkarian AV, Hodge CJ Jr (1990) Ventrolateral and dorsolateral ascending spinal cord pathway influence on thalamic nociception in cat. J Neurophysiol 64(5):1400–1412
14. Craig AD, Bushnell MC, Zhang ET, Blomqvist A (1994) A thalamic nucleus specific for pain and temperature sensation. Nature 372(6508):770–773
15. Greenspan JD, Ohara S, Sarlani E, Lenz FA (2004) Allodynia in patients with post-stroke central pain (CPSP) studied by statistical quantitative sensory testing within individuals. Pain 109(3):357–366
16. Denk F, McMahon SB, Tracey I (2014) Pain vulnerability: a neurobiological perspective. Nat Neurosci 17(2):192–200
17. Sprenger T, Seifert CL, Valet M, Andreou AP, Foerschler A, Zimmer C et al (2012) Assessing the risk of central post-stroke pain of thalamic origin by lesion mapping. Brain 135(Pt 8):2536–2545
18. Kalita J, Kumar B, Misra UK, Pradhan PK (2011) Central post stroke pain: clinical, MRI, and SPECT correlation. Pain Med 12(2):282–288
19. Krause T, Brunecker P, Pittl S, Taskin B, Laubisch D, Winter B et al (2012) Thalamic sensory strokes with and without pain: differences in lesion patterns in the ventral posterior thalamus. J Neurol Neurosurg Psychiatry 83(8):776–784
20. Symonds LL, Gordon NS, Bixby JC, Mande MM (2006) Right-lateralized pain processing in the human cortex: an fMRI study. J Neurophysiol 95(6):3823–3830
21. Wasserman JK, Koeberle PD (2009) Development and characterization of a hemorrhagic rat model of central post-stroke pain. Neuroscience 161(1):173–183
22. Yang JW, Shih HC, Shyu BC (2006) Intracortical circuits in rat anterior cingulate cortex are activated by nociceptive inputs mediated by medial thalamus. J Neurophysiol 96(6):3409–3422
23. Llinas RR, Ribary U, Jeanmonod D, Kronberg E, Mitra PP (1999) Thalamocortical dysrhythmia: a neurological and neuropsychiatric syndrome characterized by magnetoencephalography. Proc Natl Acad Sci U S A 96(26):15222–15227
24. Shyu BC, Vogt BA (2009) Short-term synaptic plasticity in the nociceptive thalamic-anterior cingulate pathway. Mol Pain 5:51
25. Walton KD, Llinas RR (2010) Central pain as a thalamocortical dysrhythmia: a thalamic efference disconnection? In: Kruger L, Light AR, Walton K (eds) Translational pain research. CRC Press, Boca Raton, pp 301–314
26. Llinas R, Urbano FJ, Leznik E, Ramirez RR, van Marle HJ (2005) Rhythmic and dysrhythmic thalamocortical dynamics: GABA systems and the edge effect. Trends Neurosci 28:325–333
27. Lenz FA, Kwan HC, Dostrovsky JO, Tasker RR (1989) Characteristics of the bursting pattern of action potentials that occurs in the thalamus of patients with central pain. Brain Res 496:357–360
28. Jeanmonod D, Magnin M, Morel A (1993) Thalamus and neurogenic pain: physiological, anatomical and clinical data. Neuroreport 4:475–478

29. Sarnthein J, Stern J, Aufenberg C, Rousson V, Jeanmonod D (2006) Increased EEG power and slowed dominant frequency in patients with neurogenic pain. Brain 129:55–64
30. Farber K, Kettenmann H (2006) Functional role of calcium signals for microglial function. Glia 54:656–665
31. Miras-Portugal MT, Diaz-Hernandez M, Giraldez L, Hervas C, Gomez-Villafuertes R, Sen RP et al (2003) P2X7 receptors in rat brain: presence in synaptic terminals and granule cells. Neurochem Res 28:1597–1605
32. Ireland MF, Noakes PG, Bellingham MC (2004) P2X7-like receptor subunits enhance excitatory synaptic transmission at central synapses by presynaptic mechanisms. Neuroscience 128:269–280
33. Alloisio S, Cervetto C, Passalacqua M, Barbieri R, Maura G, Nobile M et al (2008) Functional evidence for presynaptic P2X7 receptors in adult rat cerebrocortical nerve terminals. FEBS Lett 582:3948–3953
34. Peng W, Cotrina ML, Han X, Yu H, Bekar L, Blum L et al (2009) Systemic administration of an antagonist of the ATP-sensitive receptor P2X7 improves recovery after spinal cord injury. Proc Natl Acad Sci U S A 106:12489–12493
35. Sarnthein J, Jeanmonod D (2008) High thalamocortical theta coherence in patients with neurogenic pain. Neuroimage 39:1910–1917
36. Stern J, Jeanmonod D, Sarnthein J (2006) Persistent EEG overactivation in the cortical pain matrix of neurogenic pain patients. Neuroimage 31:721–731
37. Lu Y, Zheng J, Xiong L, Zimmermann M, Yang J (2008) Spinal cord injury-induced attenuation of GABAergic inhibition in spinal dorsal horn circuits is associated with down-regulation of the chloride transporter KCC2 in rat. J Physiol 586:5701–5715
38. Kuan YH, Shih HC, Lu HC, Tang SC, Jeng JS, Shyu BC (2015) Animal models of central poststroke pain. Rec Dev Pain Res 2:1–18
39. Kuan YH, Shih HC, Tang SC, Jeng JS, Shyu BC (2015) Targeting P_2X_7 receptor for the treatment of central post-stroke pain in a rodent model. Neurobiol Dis 78:134–145
40. Kuan YH, Shyu BC (2016) Nociceptive transmission and modulation via P2X receptors in central pain syndrome. Mol Brain 9(1):58
41. Shih HC, Kuan YH, Shyu BC (2017) Targeting brain-derived neurotrophic factor in the medial thalamus for the treatment of central poststroke pain in a rodent model. Pain 158(7):1302–1313